Affinity of Stat2 for the Subunits of the Interferon Alpha Receptor†

Abu Z. M. Saleh,‡ Vinh-Phúc Nguyen,‡ and John J. Krolewski*,‡,§

Department of Pathology and Chao Family Comprehensive Cancer Center, College of Medicine, University of California, Irvine, Irvine, California 92697-4800

Received April 2, 2002; Revised Manuscript Received July 16, 2002

ABSTRACT: The interferon alpha receptor is composed of two subunits: IFNaR1 and IFNaR2. Interferon alpha binding to the receptor induces phosphorylation of tyrosine 466 on IFNaR1, which in turn binds the SH2 domain of the latent transcription factor Stat2 to initiate signaling. Stat2 also binds to IFNaR2 in a constitutive, phosphorylation-independent manner. To explore the function of the Stat2−IFNaR2 interaction and its possible relationship to the SH2-dependent docking of Stat2 to phosphorylated IFNaR1, the affinity of Stat2 for each of the receptor subunits was determined. Recombinant proteins corresponding to the cytoplasmic domains of the receptor subunits and the central core region of Stat2 were partially purified and used in affinity precipitation experiments to demonstrate that Stat2 binds more avidly to IFNaR2 than to phosphorylated IFNaR1. Surface plasmon resonance based biosensor analysis confirmed this finding; Stat2 bound IFNaR2 (K_d = 45 nM) approximately 6-fold stronger than it bound tyrosine 466-phosphorylated IFNaR1 (K_d = 245 nM). Affinity precipitation experiments involving all three proteins (Stat2, phosphorylated IFNaR1, and IFNaR2) indicated that the Stat2−receptor interactions are independent of one another. The relevance of these data to possible models of interferon alpha signal transduction is discussed.

The interferons, members of the family of helical cytokines (*1*), induce antiviral, antiproliferative, and immunomodulatory effects on cells. These effects are mediated by the specific interaction of interferons with their cognate cell surface receptors (*2*−*5*). The receptor for interferon alpha (IFNα)[1] consists of two transmembrane proteins, IFNaR1 (*6*) and IFNaR2 (*7*, *8*), which heterodimerize following ligand binding. Tyk2 and Jak1 are Janus (JAK) family tyrosine kinases (*9*) that constitutively associate with the IFNaR1 and IFNaR2 subunits, respectively (*10*−*13*). Receptor heterodimerization activates the associated JAKs, which phosphorylate the receptors on tyrosine residues. Tyrosine 466 (Y466) on IFNaR1 is apparently the primary site of this phosphorylation, although tyrosine 481 on the same subunit may be phosphorylated to a lesser extent (*14*, *15*). The extent of IFNaR2 tyrosine phosphorylation is less certain.

Phosphorylated tyrosine 466 facilitates the activation of Stat1 and Stat2, members of a family of latent transcription factors (*16*). Specifically, Stat2 is recruited to the phosphorylated Y466 residue on IFNaR1 via its SH2 domain (*14*). Once docked, Stat2 is phosphorylated at a conserved tyrosine residue near the carboxy terminus, and it subsequently acts to recruit Stat1 to the receptor complex via a "daisy-chain" mechanism (*17*). Stat3 and Stat4 can apparently substitute for Stat1 in some circumstances (*18*). Once Stat1 is tyrosine phosphorylated, the two STAT proteins heterodimerize by reciprocal SH2−phosphotyrosine interactions (*19*), translocate to the nucleus, and, in conjunction with IRF-9, bind a specific enhancer element and stimulate gene transcription.

It has also been shown that Stat2 interacts with the cytoplasmic domain of the IFNaR2 receptor subunit (*20*, *21*). However, in contrast to the Stat2−IFNaR1 interaction, this binding is constitutive and phosphotyrosine independent (*22*). It has been proposed that this constitutive interaction of Stat2 with IFNaR2 might enhance subsequent ligand-mediated binding of Stat2 with phosphorylated IFNaR1, perhaps by increasing the local concentration of Stat2 at the cell surface (so-called predocking mechanism) (*21*). Thus, we hypothesized that Stat2 might bind phosphorylated IFNaR1 more avidly than it binds IFNaR2, thereby facilitating the movement of Stat2 from the predocking site on IFNaR2 to the productive docking site at Y466 of IFNaR1. To test this possible role for the Stat2−IFNaR2 complex, we have determined the affinity of Stat2 for each of the receptor subunits using surface plasmon resonance (SPR) technology. Unexpectedly, we found that Stat2 binds IFNaR2 with a greater affinity than it binds phosphorylated IFNaR1. Furthermore, we were unable to detect the formation of a ternary complex consisting of Stat2, IFNaR1, and IFNaR2. These data, in conjunction with our recent functional studies (*22*), argue against the predocking model and indicate that IFNaR2 binding of Stat2 might serve some other, as yet undefined, role in IFNα signaling.

† This work was supported by a research grant (RG-2928A1-T) from the National Multiple Sclerosis Society, as well as by funds from the National Institutes of Health (CA56862). V.-P.N. is supported by an institutional training grant from the National Cancer Institute (CA09054).

* To whom correspondence should be addressed. Tel: 949-824-4089. Fax: 949-824-2160. E-mail: jkrolews@uci.edu.

‡ Department of Pathology.

§ Chao Family Comprehensive Cancer Center.

[1] Abbreviations: IFNα, interferon alpha; JAK, Janus family kinase; GST, glutathione *S*-transferase; IPTG, isopropyl 1-thio-β-D-galactopyranoside; MBP, maltose binding protein; HSB, 10 mM HEPES (pH 7.4), 150 mM NaCl, 3 mM EDTA, and 0.005% P-20; mAb, monoclonal antibody; SPR, surface plasmon resonance; RU, resonance units.

10.1021/bi025913f CCC: $22.00
Published on Web 08/21/2002

MATERIALS AND METHODS

Antibodies. PY20 (Transduction Laboratories), a mouse monoclonal antibody (mAb) directed against phosphotyrosine, was used at 1:1000 dilution in immunoblotting experiments and 1:333 dilution in immunoprecipitation experiments. Rabbit polyclonal antibodies against glutathione *S*-transferase (GST) (B-14) and hexahistidine (H-15), from Santa Cruz Biotechnology, were used at 1:5000 and 1:1000 dilution, respectively, in immunoblotting experiments. A separate goat polyclonal anti-GST antibody (BIAcore) was employed in the surface plasmon resonance experiments.

Recombinant DNA Constructs. To produce a fragment of the human Stat2 protein spanning residues 136−702, the corresponding cDNA was PCR amplified using *Pfu* polymerase (Stratagene) and the deoxyoligonucleotide primers 5′-ATGTGACTCGAGGAAACACCTGTGGA and 5′-GGATCCTCGAGTTACTGTCTATTAGAGA. The resulting 1.7 kb fragment was restriction digested, cloned into the *Xho*I site of pET15b (Novagen), a T7 polymerase regulated expression vector that encodes hexahistidine and thrombin recognition sequences at the amino terminus of the resulting protein, and sequenced. A plasmid encoding the maltose binding protein (MBP) was fused to a part of the cytoplasmic domain of the human IFNaR2 gene spanning amino acids 260−498 by amplifying the appropriate cDNA using the *Pfu* polymerase and the deoxyoligonucleotide primers 5′-GCAGAATTCAGCACCATAGTGACACTG and 5′-AGGAAGCTTCTTAATCAGATGGAGCATC. The product was restriction digested, ligated into the *Eco*RI and *Hin*dIII sites of pMAL-c2 (New England Biolabs), and sequenced. Plasmids expressing GST fused to a portion of the cytoplasmic domain of the human IFNaR1 receptor subunit corresponding to residues 460−486 [GST−IFNaR1 (460−486) as well as the corresponding Y466F and Y481F mutants] have been described previously (*14*). Similar GST fusion constructs encoding residues 340−462 of the cytoplasmic domain of human IFNaR2 [GST-IFNaR2 (340−462)], as well as the m1 mutant version, in which DDED at residues 435−438 has been converted to AAAA, have also been described (*22*).

Purification of Recombinant Proteins. A 3 L culture of *Escherichia coli* BL21(λDE3) expressing recombinant 6×His-Stat2 (136−702) protein was grown at 37 °C to mid-log phase, induced with 0.4 mM isopropyl 1-thio-β-D-galactopyranoside (IPTG), and grown an additional 4 h at 30 °C. Cells were centrifuged, resuspended in 50 mL of 25 mM sodium phosphate (pH 7.2), 25 mM KCl, 10 mM 2-mercaptoethanol, and 5% glycerol, treated with 200 μg/mL lysozyme for 30 min at 4 °C, freeze−thawed, and sonicated. Lysates were centrifuged at 96000*g* for 1 h, the supernatant was applied to a 5 mL HTP hydroxylapatite column (Bio-Rad), and bound proteins were eluted by a linear 25−400 mM sodium phosphate (pH 6.8) gradient. Fractions were analyzed by SDS−PAGE followed by Coomassie blue staining, and those containing recombinant protein were pooled, dialyzed against 20 mM sodium phosphate (pH 7.8), 500 mM NaCl, and 10 mM 2-meraptoethanol, and applied to a 0.75 mL nickel resin (Invitrogen) column. The column was subjected to successive washes (at pH 6.0) containing 0, 10, and 50 mM imidazole, and recombinant protein was eluted with 150 mM imidazole, dialyzed, and (in some cases) digested with biotinylated thrombin (Novagen) overnight at 4 °C to remove the hexahistidine tag at the amino terminus. After the thrombin was captured on strepavidin beads, the cleaved recombinant Stat2 (residues 136−702, plus the amino acids Gly-Ser-His-Met-Leu-Glu at the extreme amino terminus) was reapplied to a nickel resin column, and the flow-through was collected and dialyzed exhaustively against 10 mM HEPES (pH 7.4), 150 mM NaCl, 3 mM EDTA, and 0.005% P-20 (HSB). Protein was concentrated by Centricon-30 (Amicon) centrifugation, the concentration was determined using a commercial Bradford reagent (Bio-Rad), and the final preparation was stored at −20 °C.

GST−IFNaR2 (340−462) fusion proteins were prepared by transforming appropriate plasmids into *E. coli* BL21-codon plus (λDE3)-RP (Stratagene). Bacterial cultures were induced and lysed as described above. The cleared lysate was loaded on a Mono-Q column (Bio-Rad), and bound proteins were eluted by a linear 25−500 mM KCl gradient. Fractions containing recombinant protein were pooled and dialyzed against lysis buffer, loaded on a 1 mL glutathione−agarose (Sigma) column, and eluted with 10 mM glutathione. Appropriate fractions were pooled and further purified by gel filtration chromatography on Sepharose CL-6B (Sigma). Purified protein was dialyzed into HBS. Protein concentration determination and storage were performed as described above. Tyrosine-phosphorylated recombinant GST−IFNaR1 (460−486) protein was produced by a similar protocol, except that the appropriate cDNA was transformed into *E. coli* BL21(λDE3) TKB1 (Stratagene), which constitutively expresses the kinase domain of the *elk* tyrosine kinase. MBP−IFNaR2 (260−498) protein lysates were prepared by introducing the appropriate plasmid into *E. coli* BL21(λDE3) and then inducing and lysing cultures as described above. Cleared lysates were stored at −80 °C.

Protein Precipitation and Immunoblotting. For immunoprecipitations, aliquots of GST−IFNaR1 recombinant protein were diluted into 1 mL of phosphate-buffered saline (PBS) containing 1% NP-40 and incubated with 3 μL of PY20 mAb for 1 h at 4 °C, with tumbling. An aliquot (40 μL) of protein A−Sepharose beads (Sigma) was added to each reaction, the mixture was tumbled for an additional 1 h, and bead−protein complexes were washed extensively with the same buffer and eluted with sample buffer. For affinity precipitations, GST, MBP, or fusion protein(s) was (were) similarly diluted into PBS/NP-40 and incubated with either 40 μL of glutathione−agarose beads or 40 μL of amylose−agarose beads, as required, for 30 min at 4 °C with tumbling. Complexes were washed as above, recombinant 6×His-Stat2 was added, and following further tumbling for 1 h at 4 °C, the complexes were washed and eluted with sample buffer. SDS−PAGE electrophoresis, immunoblotting, protein detection by chemiluminescence, and densitometry were carried out as previously described (*22*, *23*).

Surface Plasmon Resonance Analysis. SPR measurements were made on a Model X biosensor (BIAcore). All reactions were carried out in HBS. Approximately 8000 resonance units (RU) of anti-GST antibody was immobilized to each of two flow cells on a CM5 biosensor chip (BIAcore), according to the manufacturer's instructions, using supplied reagents. For each measurement, ∼140 RU of GST-fused protein was bound (as ligand) to the CM5-linked anti-GST antibody (1 RU = 1 pg of protein/mm^2) to the experimental flow cell. Association phase data were obtained by injecting

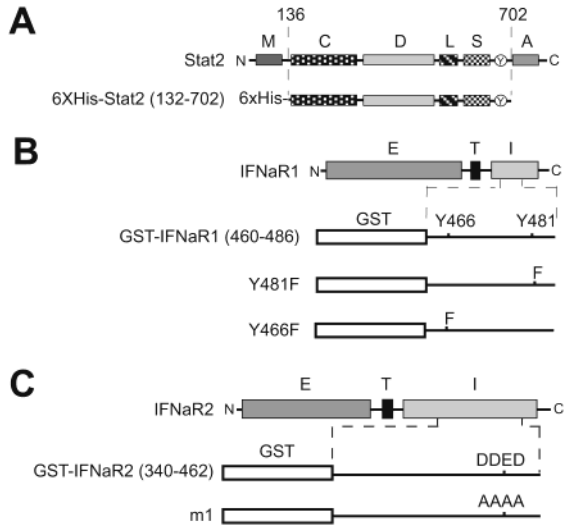

FIGURE 1: Schematic diagrams of recombinant proteins. (A) Domain structure of Stat2 recombinant protein spanning residues 136−702 of the native protein. Functional domains are indicated as follows: 6×His, hexahistidine sequence employed in purification; M, enhancer element multimerization domain; C, coiled-coil domain; D, dimerization domain; L, linker domain; S, SH2 domain; Y (inside circle), tyrosine phosphorylation site; A, transcriptional activation domain. (B) Structure of GST−IFNaR1 recombinant fusion proteins spanning residues 460−486. The E, extracellular, T, transmembrane, and I, intracellular, or cytoplasmic domains of the native IFNaR1 receptor subunit are shown on the top line. The second line shows the extent of the recombinant wild-type protein fragment, along with the location of IFNaR1 tyrosine residues and the GST moiety (open rectangle). The third and fourth lines indicate the structure of the corresponding IFNaR1 mutants. (C) Structure of GST−IFNaR2 recombinant fusion proteins spanning residues 340−462. Similar to (B), except that the location of the m1 mutant version, in which DDED is converted to AAAA (residues 435−438), is shown.

various concentrations of recombinant Stat2 over both flow cells (in series) at a flow rate of 20 μL/min for 2 min. Dissociation phase data were acquired while buffer flowed past the sensor chip at the same flow rate. After each interaction cycle, the surface was regenerated by injection of 10 μL of 10 mM glycine (pH 2.2) to release the bound ligand (GST) protein. The response from the reference surface was subtracted to correct for refractive index changes and for nonspecific binding. Equilibrium and kinetic rate constants were obtained by analyzing the data using BIA evaluation software version 2.1 (BIAcore) employing a 1:1 Langmuir binding model. χ^2 values of <10 are indicative of a good fit.

RESULTS

Purification and Characterization of Recombinant Proteins. Recombinant proteins corresponding to the central core of Stat2 (residues 136−702; Figure 1A), as well as GST fusion proteins encoding the Stat2 binding domains of the two IFNα receptor subunits (Figure 1B,C), were partially purified from bacteria and employed in the various protein−protein binding experiments described below. In the case of Stat2, we expressed and purified the fragment spanning residues 136−702 because it has been shown that a homologous region of Stat1 can be recovered in a soluble fraction from bacterial lysates and, when tyrosine phosphorylated, binds DNA (*24*). This same region of Stat1 is resistant to limited proteolysis, consistent with crystallographic data indicating that this protein fragment contains a central hydrophobic core such that the various conserved domains (e.g., SH2) do not appear to fold into completely distinct modules (*24*, *25*). We have previously demonstrated that the 136−702 fragment binds efficiently to IFNaR2 (*22*). The IFNaR1 and IFNaR2 constructs correspond to portions of the intracellular domains that we have shown confer maximal binding to Stat2 (*14*, *22*, *26*).

The recombinant Stat2 protein was engineered to contain a hexahistidine tag near the amino terminus and purified by successive hydroxylapatite and nickel resin chromatography steps. This protein, with an intact hexahistidine sequence, was used in the affinity precipitation studies. Because the hexahistidine tag produced high background binding in preliminary SPR analyses, we cleaved the tag with thrombin and rechromatographed the digested material on the nickel resin column. Aliquots of the flow-through were assessed by Coomassie blue staining of SDS−acrylamide gels (Figure 2A). Examination of serial dilutions of the purified material (data not shown) revealed a purity of >90%. Recombinant proteins encoding portions of the IFNaR1 and IFNaR2 cytoplasmic domains were purified by Mono-Q and glutathione−agarose chromatography steps, followed by gel filtration. The GST moiety was not cleaved from the recombinant proteins, allowing for affinity precipitation by glutathione−agarose beads and capture by anti-GST antibodies on the SPR biosensor chips (see below). Coomassie blue staining of SDS−polyacrylamide gels of these purified fusion proteins is shown in Figure 2B; comparison of serial dilutions revealed >85% purity for each of these proteins (data not shown). It has been reported that GST proteins form dimers (*27*). We confirmed this for the proteins in Figure 2B by analytical gel filtration of the purified GST fusion proteins, employing unfused GST, lysozyme, and bovine serum albumin as standards (data not shown). Thus, higher order aggregates, which might complicate the interpretation of the binding experiments shown below, were not detectable in these protein preparations.

Stat2 binds only to the tyrosine phosphorylated form of IFNaR1. To produce phosphorylated recombinant protein, GST−IFNaR1 constructs were transformed into an *E. coli* strain (TKB1) expressing the tyrosine kinase domain of the human receptor-type tyrosine kinase *elk*. The fragment of the IFNaR1 cytoplasmic domain employed in these studies contains two tyrosine residues, corresponding to residues 466 and 481 of the wild-type, full-length protein. Figure 2C shows that the wild-type and 481F variants of recombinant GST−IFNaR1 proteins were readily detected in PY20 anti-phosphotyrosine immunoblots of the partially purified proteins, while the 466F mutant was only partially phosphorylated. The 466F/481F double mutant was not detectably phosphorylated. This pattern, of phosphorylation predominantly on Y466, is essentially identical to the pattern we previously observed either when IFNaR1 proteins were tyrosine phosphorylated by JAK family kinases in vitro (*11*, *14*) or when phosphorylation was induced in vivo by dimerizing a CD4−IFNaR1 chimera (*15*). This pattern of phosphorylation (Y466 > Y488) completely correlates with the pattern of Stat2 SH2-mediated docking site usage in response to IFNα (*14*). However, the in vivo pattern of

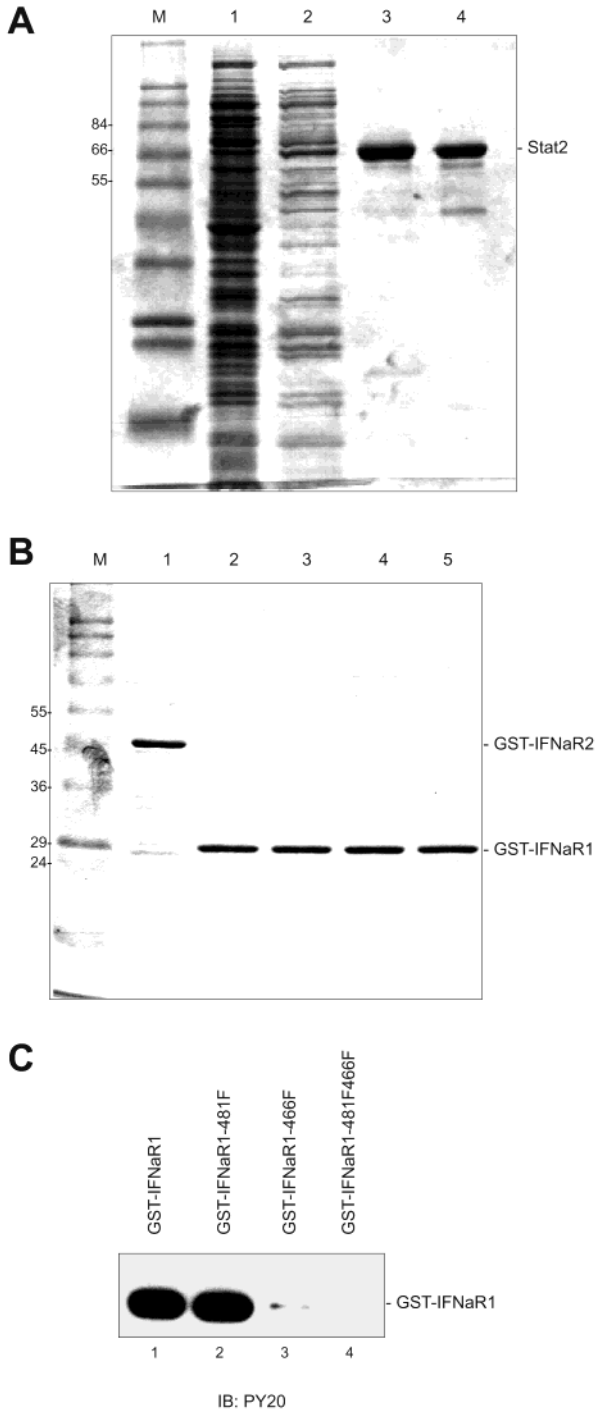

FIGURE 2: Characterization of partially purified recombinant proteins. (A) Coomassie blue stained SDS−PAGE of samples from various steps in the purification of Stat2 (136−702). Key: M, molecular mass standards (mass of relevant standards are indicated); lane 1, cleared cell lysate; lane 2, HTP hydroxylapatite column eluent; lane 3, nickel resin column eluent; lane 4, second nickel resin column flow-through. (B) Coomassie blue stained SDS−PAGE of partially purified GST−IFNaR2 (340−462) and GST−IFNaR1 (460−486) proteins, following Mono-Q, glutathione−agarose, and gel filtration chromatography steps. Key: M, molecular mass standards (mass of relevant standards are indicated); lane 1, GST−IFNaR2 (340−462); lane 2, IFNaR1 (460−486); lane 3, GST−IFNaR1 (460−486) 481F; lane 4, GST−IFNaR1 (460−486) 466F; lane 5, GST−IFNaR1 (460−486) 466F/481F. (C) PY20 (anti-phosphotyrosine antibody) immunoblot of purified IFNaR1 proteins (as indicated).

IFNaR1 phosphorylation in response to IFNα has not been determined.

To obtain meaningful data on the affinity of Stat2 for phosphorylated IFNaR1, it is necessary to use recombinant GST−IFNaR1 that is stoichiometrically phosphorylated. When Stat3 was coexpressed in the *E. coli* TKB1, it was tyrosine phosphorylated at essentially 100% efficiency (*28*), suggesting that this approach can indeed produce fully phosphorylated protein. The method outlined in Figure 3A was utilized to determine if IFNaR1 is phosphorylated to a similar extent. Various amounts of tyrosine-phosphorylated GST−IFNaR1 481F protein (which contains a single tyrosine residue, Y466, in the IFNaR1 portion) were fractionated by SDS−PAGE and transferred to nitrocellulose membranes to generate two identical filters (Figure 3A, T1 and T2). An analogous set of filters (Figure 3A, P1 and P2), containing 100% tyrosine-phosphorylated protein, were generated by fractionating PY20 immunoprecipitates of the same protein. The filters were probed with PY20 and anti-GST, as indicated in Figure 3A, to determine the amount of tyrosine phosphorylated and total protein, respectively, on the appropriate filters. Blot signals were quantitated by densitometry, and the slopes of the resulting plots of optical density vs protein concentration were used to calculate phosphorylation efficiency. The ratio of the slopes derived from the two PY20 immunoblots (S1 and S2), normalized for total protein using the data from the anti-GST immunoblots (S3 and S4), yields a relative phosphorylation efficiency of 1.05 (Figure 3B), consistent with complete phosphorylation of tyrosine 466.

In contrast to IFNaR1, Stat2 binds IFNaR2 constitutively and requires neither receptor nor STAT phosphorylation (*22*). Furthermore, the interaction is partially disrupted if a conserved stretch of acidic amino acids is converted to alanine, suggesting that the interaction between these proteins may be ionic. To test this, 6×His-Stat2 protein was affinity precipitated by GST−IFNaR2 (340−462) in the presence of various concentrations of NaCl (Figure 4). Immunoblotting of protein complexes collected on glutathione−agarose beads with an antibody directed against the hexahistidine sequence revealed a decrease in Stat2 binding with increasing salt concentration, consistent with an ionic interaction.

Comparative Affinity Precipitation of Stat2 by GST-Linked Receptor Cytoplasmic Domains. As an initial approach to determine the relative affinities of the cytoplasmic Stat2 binding domains of IFNaR1 and IFNaR2, we performed affinity precipitation experiments at two concentrations of Stat2 (Figure 5). Similar to Figure 4, a large excess of GST fusion protein containing portions of the cytoplasmic domains of the receptor subunits was bound to glutathione−agarose beads, incubated with either 0.9 or 11.7 nM hexahistidine-tagged Stat2 (136−702), and immunoblotted. Although IFNaR2 fusions were clearly able to affinity precipitate Stat2 at the lower input concentration (Figure 5A), the interaction with tyrosine-phosphorylated IFNaR1 was only detected at the higher Stat2 input concentration (Figure 5B), suggesting that Stat2 binds IFNaR2 with higher affinity. Stat2 binding to IFNaR1 correlated tightly with tyrosine phosphorylation at Y466 (compare Figures 2C and 5). As observed previously, mutation to alanine of the DDED sequence at residues 435−438 of IFNaR2 (Figure 6B, lane 6) significantly reduced, but did not completely obliterate, Stat2 binding (*22*).

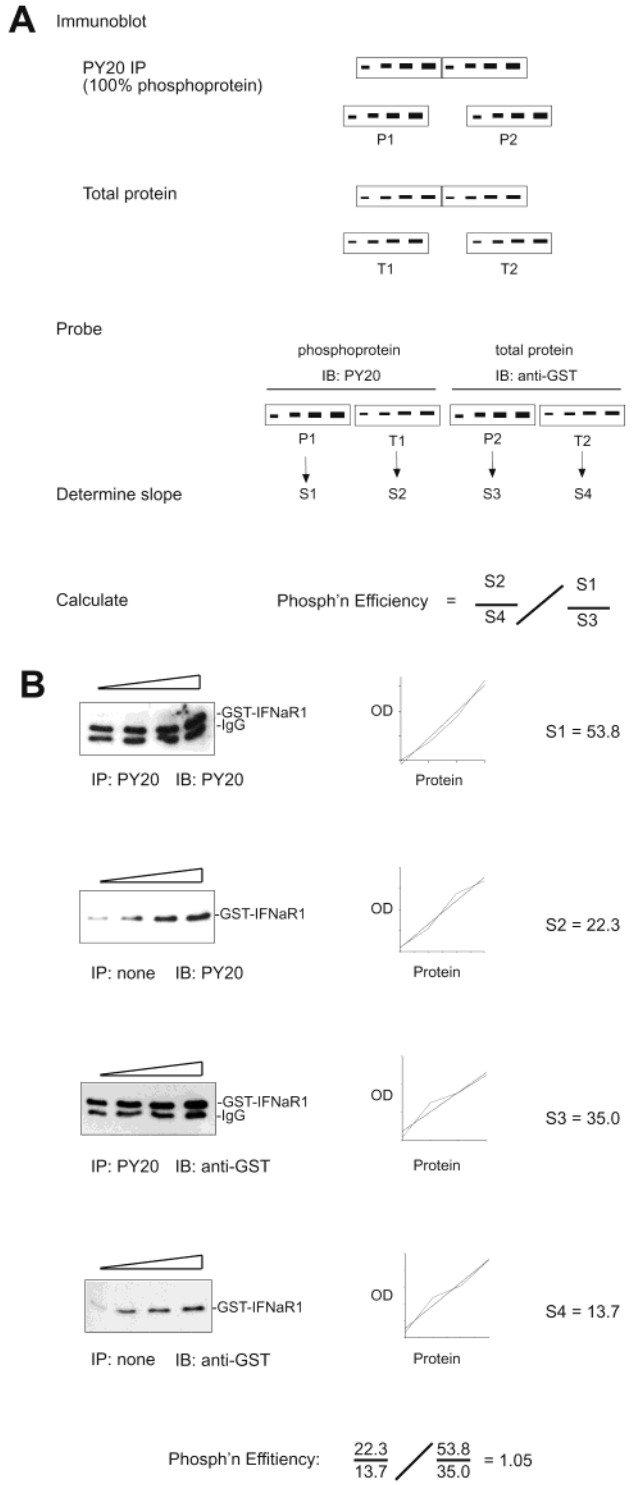

FIGURE 3: Recombinant IFNaR1 protein is stoichiometrically tyrosine-phosphorylated. (A) Schematic of the experimental approach as detailed in the text. (B) Determination of phosphorylation efficiency. The left column contains immunoblots of various amounts of either unfractionated (IP: none) or anti-phosphotyrosine antibody immunoprecipitated (IP: PY20) phosphorylated GST−IFNaR1 (460−486) 481F protein, immunoblotted with either PY20 or anti-GST antibodies, to detect phosphorylated or total protein, respectively. Each blot image was scanned, the optical density of each band was plotted against the amount of input protein, and the slope of the linear regression line was determined. Using the formula illustrated in panel A, the phosphorylation efficiency was determined.

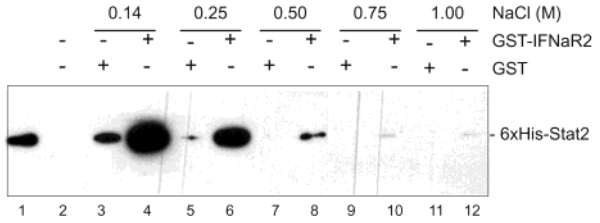

FIGURE 4: The binding of Stat2 to IFNaR2 is salt dependent. An excess (∼2.5 μg) of purified GST or GST−IFNaR2 (340−462) fusion protein was precipitated with glutathione−agarose beads and incubated with 6×His-Stat2 (136−702) (12 nM final concentration) in a buffer containing NaCl at the concentration indicated across the top of the figure. The resulting protein complexes were precipitated and subjected to SDS−PAGE, and 6×His-Stat2 (136−702) was detected by immunoblotting with anti-hexahistidine antibody. Lane 1 contains a small amount of purified protein (∼5% of the amount used in the binding assays) to serve as a size standard and blot control. Ponceau S red staining of the blot filter revealed that lanes 2−12 contained the same amount of GST or GST fusion protein (data not shown).

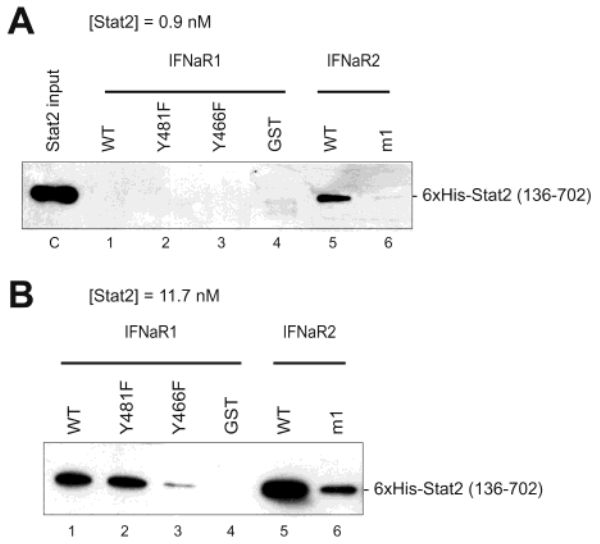

FIGURE 5: Affinity precipitation of Stat2 by IFNaR1 and IFNaR2 cytoplasmic domains. Similar to Figure 4, equivalent amounts (∼2.5 μg) of various versions of phosphorylated GST−IFNaR1 (460−486), GST−IFNaR2 (340−462), or GST alone (as indicated across the top of each panel) were bound to glutathione−agarose beads and then incubated with 6×His-Stat2 (136−702) at a final concentration of 0.9 nM (A) or 11.7 nM (B). The resulting protein complexes were precipitated and subjected to SDS−PAGE, and 6×His-Stat2 (136−702) was detected by immunoblotting with anti-hexahistidine antibody. Lane C contains the input amount of Stat2 (63 ng). Ponceau S red staining of the blot filter revealed that each of the numbered lanes in both panels contained the same amount of GST or GST fusion protein (data not shown).

Densitometry revealed that Stat2 bound IFNaR2 about 4-fold more avidly than phosphorylated IFNaR1 (data not shown).

SPR Biosensor Analysis of the Stat2−Receptor Interactions. To confirm the results seen in Figure 5 and determine the affinity constants for these two Stat2−receptor interactions, we employed SPR-based biosensor analysis (*29*, *30*). To perform these measurements, an excess of anti-GST antibody was bound to a carboxymethyldextran sensor chip and used to immobilize GST fusion proteins encoding portions of the receptor cytoplasmic domains. We chose this experimental design to ensure that the relevant binding surface of the protein immobilized on the sensor chip is presented in a uniform, vectorial configuration, readily

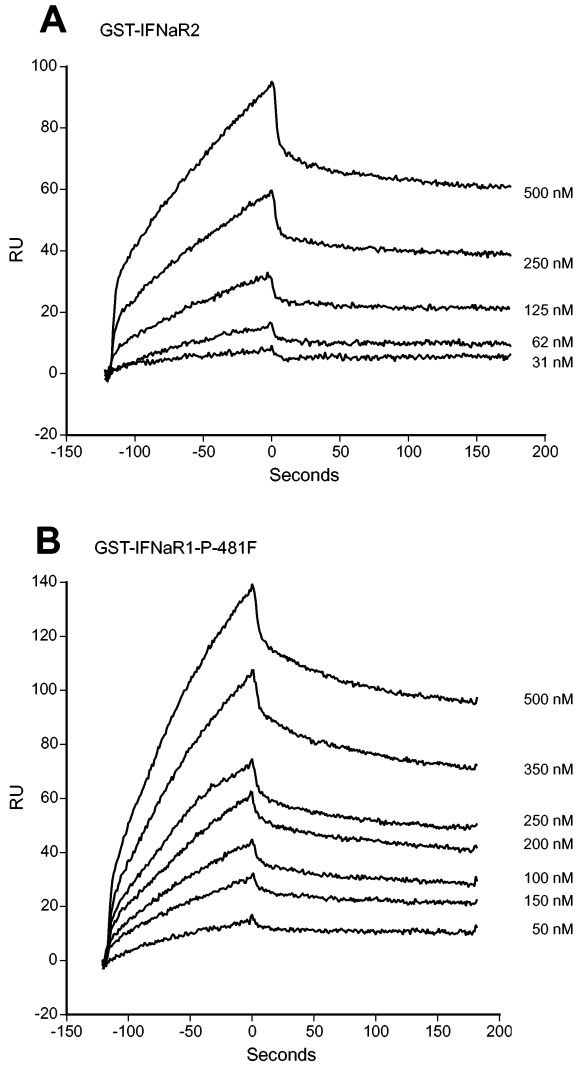

FIGURE 6: Sensorgrams of Stat2 binding to IFNaR1 and IFNaR2. Partially purified GST−IFNaR2 (340−462) (A) and phosphorylated GST−IFNaR1 (460−486) 481F (B) were bound to anti-GST antibody which has been covalently linked to dextran-coated sensor chips. Partially purified Stat2 (136−702) was flowed past the sensor chip at 20 μL/min at the indicated concentrations (right side), and SPR was measured. Plots of reference cell subtracted sensorgrams (RU vs time in seconds) (wavy lines) are shown for each protein combination.

accessible for interaction with the protein that flows over the surface. Various concentrations of recombinant Stat2 (136−702) protein were injected, and the interaction was monitored by measuring SPR vs time (Figure 6). Relatively low levels of GST fusion protein were immobilized on the sensor chips to ensure that the kinetic measurements were made in the linear range and relatively high flow rates were used to minimize mass transport effects on the measurements. The data from the sensorgrams shown in Figure 6 were used to solve the predicted pseudo-first-order rate equations utilized to model SPR analysis in flow cells (*31*). The results, including association and dissociation rates, K_d, and χ^2, an estimate of the error in the curve-fitting process, are listed in Table 1. Each of the analyses was performed in duplicate, with good agreement between replicates. Similar to the affinity precipitation data in Figure 5, the recombinant Stat2 fragment bound the IFNaR2 target ($K_d \sim 45$ nM) approximately 6-fold more strongly than it bound phosphorylated Y466 on IFNaR1 ($K_d \sim 245$ nM). It is of interest that most of the difference in K_d is accounted for by differences in the association rates. Stat2 bound the wild-type IFNaR1 fragment, containing Y466 and Y481 ($K_d \sim 157$ nM), somewhat more strongly than it bound the 481F mutant shown in Figure 6B (data not shown). However, the significance of this measurement is unclear, as the wild-type protein is apparently partly phosphorylated on Y481 (Figure 2C), which is a weak docking site for Stat2 (*14*, *15*). Thus, Stat2 may bind to two sites on some molecules of the wild-type IFNaR1 fragment. Since we employed a 1:1 stoichiometry in the model used to calculate K_d, our curve fitting for this particular construct may not be valid. Finally, Stat2 did not show detectable binding to GST−IFNaR1 466F, GST−IFNaR1 481F/466F, or GST alone at the highest Stat2 concentration tested (data not shown).

Table 1: Rate and Equilibrium Dissociation Values for Stat2 Interactions

ligand	k_a (M^{-1} s^{-1}) × 10^{-4}	k_d (s^{-1}) × 10^4	K_d (nM)	χ^2
GST−IFNaR2	1.62	7.8	48	1.36
(340−462)	1.90	8.3	42	4.68
GST−IFNaR1	0.53	11.1	210	2.67
(460−486) PY466	0.44	12.3	281	3.22

Stat2, IFNaR1, and IFNaR2 Do Not Form a Ternary Complex. A possible alternative to the predocking mechanism described above is a mechanism where Stat2 simultaneously binds to IFNaR2 and phosphorylated IFNaR1 to form a ternary complex. To test this possibility, all three proteins were incubated together and then subjected to affinity precipitation for one of the proteins, followed by blotting for the other two proteins. To carry out these experiments, we replaced GST−IFNaR2 with a version of IFNaR2 fused to the maltose binding protein (MBP) to enable us to differentiate each of the three recombinant proteins. MBP−IFNaR2 was bound to amylose−agarose beads and incubated with a mixture of hexahistidine-tagged Stat2 and phosphorylated GST−IFNaR1, and the resulting protein complexes were precipitated by centrifugation and transferred to a blotting membrane (Figure 7). The Ponceau S red staining showed that equal amounts of MBP−IFNaR2 protein were recovered from each of the precipitates. This filter was cut in half, and the upper portion was probed with antibody against hexahistidine to detect Stat2, while the lower part was probed with anti-GST antibody to detect phosphorylated IFNaR1. The immunoblot directed against recombinant Stat2 shows that, as expected, IFNaR2 binds Stat2, even in the presence of recombinant IFNaR1. However, the anti-GST immunoblot reveals that IFNaR1 did not bind to the IFNaR2−Stat2 complex (Figure 7, lane 7) nor did it bind to IFNaR2 alone (Figure 7, lane 6). Control experiments demonstrate that hexahistidine-tagged Stat2 employed in these experiments also bound phosphorylated IFNaR1 in separate glutathione−agarose affinity precipitation reactions (Figure 7, lane 9). These data support the idea that these two Stat2−receptor interactions are independent of each other.

DISCUSSION

STATs are multidomain proteins that mediate both signal transduction and gene transcription. In the best characterized

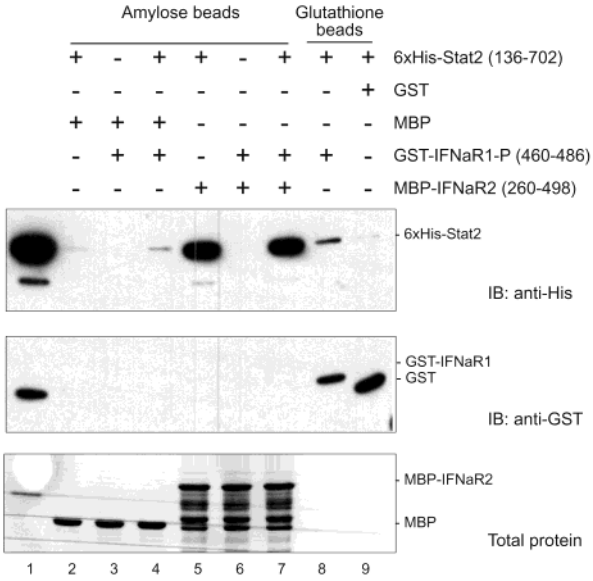

FIGURE 7: Stat2, IFNaR1, and IFNaR2 do not form a ternary complex. Approximately 2.5 μg of MBP (lanes 2−4) or MBP−IFNaR2 (260−498) (lanes 5−7) was bound to amylose−agarose beads (lanes 2−7) and then incubated with 750 ng of 6×His-Stat2 (136−702) and/or 2.5 μg of phosphorylated GST−IFNaR1 (460−486), as indicated. Similarly, 2.5 μg of GST (lane 9) or phosphorylated GST−IFNaR1 (460−486) (lane 8) was bound to glutathione−agarose beads (lanes 8 and 9) and then incubated with 750 ng of 6×His-Stat2 (136−702). The resulting protein complexes were precipitated, subjected to SDS−PAGE, and immunoblotted. Appropriate halves of the blot membrane were probed with anti-hexahistidine antibody to detect 6×His-Stat2 (136−702) (upper panel) or anti-GST antibody to detect GST−IFNaR1 (460−486) (middle panel). Lane 1 was loaded with a mixture of 150 ng of 6×His-Stat2 (136−702) and 2.5 μg of GST as blot controls. The faster migrating band in the anti-hexahistidine blot is probably a degradation product. Ponceau S red staining of the upper half of the blot filter revealed that lanes 2−7 contained similar amounts of MBP or MBP fusion protein (lower panel). The faster migrating bands in lanes 5−7 of the Ponceau S red stained membrane are degradation or premature termination products.

STAT signaling cascades, such as the pathway triggered by IFNα, STATs translocate from the cell surface to the nucleus via a series of protein−protein interactions with receptors, JAK family kinases, other STATs, and additional transcription factors, such as IRF-9. The STAT SH2 domains mediate at least two of these critical interactions: docking to the receptor and, subsequently, STAT−STAT dimerization. In contrast to many other SH2−phosphoreceptor interactions, the interaction of the Stat SH2 domain with the receptor is a relatively transient event, since signaling requires that the STAT protein "undock" from the receptor to participate in the formation of a STAT−STAT dimer. One possibility is that STAT SH2 binding to its target phosphotyrosine docking site is relatively weak compared to other SH2−phosphotyrosine interactions. Comparison of our data with that in the literature, however, suggests that this is not the case.

Specifically, for the Stat2 SH2 domain and the phosphotyrosine at position 466 of IFNaR1, we obtained a K_d of 245 nM. Although a number of initial reports indicated that the SPR-derived K_d values for typical SH2−phosphotyrosine interactions were as low as 3.5 nM (*32*), many of these measurements were probably inaccurate due to flaws in the experimental design (*33*). In particular, high levels of immobilized ligand on the sensor chip surface and the use of dimeric (GST-derived) proteins as analytes may have led to cooperative binding at the sensor chip surface resulting in spuriously high K_d values. A subsequent reassessment of these data that relied on isothermal calorimetry to confirm refined SPR data produced K_d values in the range of 300−600 nM for some well-characterized SH2 domain−phosphotyrosine motif pairs. These include src SH2/middle T phospho-Y315 and p85 SH2/PDGFR phospho-Y751 (*33*). Thus, the K_d we obtained for the Stat2 SH2−IFNaR1 phospho-Y466 interaction is similar to the values for other, typical SH2 domains. Furthermore, our K_d value is comparable to the value (137 nM) obtained for the interaction of the Stat1 SH2 domain with the phosphorylated Y440 on the interferon γ receptor α-subunit (*34*). There does seem to be a significant difference in the kinetic rate constants for STAT−SH2 domain interactions with phosphotyrosine motifs, relative to other SH2 domains. Stat2 (Table 1) and Stat1 (*34*) both have slower on and off rates compared to other SH2 domain interactions (*33*). However, the significance of this observation relative to the transient nature of the STAT−receptor interaction is unclear.

Analysis of the interaction of the Stat1 SH2 domain with the phosphorylated Y440 on the interferon γ receptor α-subunit has led to a model in which STAT activation proceeds via a sequential, affinity-driven mechanism (*34*). Support for this model comes from the observation that the affinity of STAT−STAT dimerization, driven by reciprocal SH2−phosphotyrosine interactions, is significantly greater than the affinity of the STAT protein for its cognate docking site on the receptor. Our data on the K_d for the Stat2−IFNaR1 interaction is consistent with this model, assuming all STAT−STAT dimers have comparable affinities.

We sought to test an extension of the affinity-driven signaling model, based on the suggestion by others that Stat2 binding to IFNaR2 functions as a "predocking" site for Stat2 (*21*). In particular, we reasoned that binding to the IFNaR2 subunit should have a lower affinity than binding of the Stat2 SH2 domain to the phosphorylated IFNaR1 subunit, allowing for a sequential translocation of Stat2 from predocking site to docking site to dimer and then on into the nucleus. However, as seen by both comparative affinity precipitation (Figure 5) and SPR analysis (Figure 6 and Table 1), Stat2 actually has a greater affinity for the IFNaR2 subunit than it has for phosphorylated IFNaR1. Our conclusion that a sequential, affinity-driven mechanism is not supported by our data should be tempered by our incomplete knowledge of the stoichiometry of the IFNα receptor complex. Specifically, we have generally assumed that IFNaR1 and IFNaR2 form a simple heterodimer upon ligand binding. This has not been well demonstrated experimentally, and in fact there is indirect evidence to support a more complex stoichiometry, such as a 2:1 IFNaR1:IFNaR2 complex (*2*).

As a possible alternative to the affinity-driven model, we also tested the idea that Stat2 binding to IFNaR2 might facilitate its eventual ligand-dependent binding to phosphorylated IFNaR1 by forming a ternary complex containing Stat2 and both receptor subunits. As seen in Figure 7, we are not able to detect the formation of such a ternary complex, even at relatively high protein concentrations where we can readily detect the association of Stat2 with the individual receptor subunits. In a separate, related series of experiments, we have also recently examined the functional

consequences of interrupting the interaction between Stat2 and IFNaR2. Surprisingly, we find that this interaction is dispensable for IFNα signaling (*22*). Thus, these two sets of data, both biochemical and functional, argue strongly against the predocking hypothesis. The relatively strong binding of Stat2 to the IFNaR2 receptor subunit would appear to suggest a physiologic role for this interaction, but at present this role remains unknown and is therefore the focus of ongoing research.

ACKNOWLEDGMENT

We thank Larry Vickery, Kevin Hoff, and Jonathan Silberg (University California, Irvine) for the use of, and assistance with, the BIAcore Model X instrument.

REFERENCES

1. Bazan, J. F. (1990) *Proc. Natl. Acad. Sci. U.S.A. 87*, 6934−6938.
2. Mogensen, K. E., Lewerenz, M., Reboul, J., Lutfalla, G., and Uzé, G. (1999) *J. Interferon Cytokine Res. 19*, 1069−1098.
3. Pestka, S. (1997) *Semin. Oncol. 24*, S918−S940.
4. Domanski, P., and Colamonici, O. R. (1996) *Cytokine Growth Factor Rev. 7*, 143−151.
5. Uzé, G., Lutfalla, G., and Mogensen, K. E. (1995) *J. Interferon Cytokine Res. 15*, 3−26.
6. Uzé, G., Lutfalla, G., and Gresser, I. (1990) *Cell 60*, 225−234.
7. Lutfalla, G., Holland, S. J., Cinato, E., Monneron, D., Reboul, J., Rogers, N. C., Smith, J. M., Stark, G. R., Gardiner, K., Mogensen, K. E., Kerr, I. M., and Uzé, G. (1995) *EMBO J. 14*, 5100−5108.
8. Domanski, P., Witte, M., Kellum, M., Rubinstein, M., Hackett, R., Pitha, P., and Colamonici, O. R. (1995) *J. Biol. Chem. 270*, 21606−21611.
9. Wilks, A. F., Harpur, A. G., Kurban, R. R., Ralph, S. J., Zurcher, G., and Ziemiecki, A. (1991) *Mol. Cell. Biol. 11*, 2057−2065.
10. Colamonici, O. R., Uyttendaele, H., Domanski, P., Yan, H., and Krolewski, J. J. (1994) *J. Biol. Chem. 269*, 3518−3522.
11. Yan, H., Krishnan, K., Lim, J. T. E., Contillo, L. G., and Krolewski, J. J. (1996) *Mol. Cell. Biol. 16*, 2074−2082.
12. Domanski, P., Fish, E., Naduea, O. W., Witte, M., Platanais, L. C., Yan, H., Krolewski, J., Pitha, P., and Colamonici, O. R. (1997) *J. Biol. Chem. 272*, 26388−26393.
13. Yan, H., Piazza, F. P., Krishnan, K., Pine, R., and Krolewski, J. J. (1998) *J. Biol. Chem. 273*, 4046−4051.
14. Yan, H., Krishnan, K., Greenlund, A. C., Gupta, S., Lim, J. T. E., Schreiber, R. D., Schindler, C., and Krolewski, J. J. (1996) *EMBO J. 15*, 1064−1074.
15. Krishnan, K., Yan, H., Lim, J. T. E., and Krolewski, J. J. (1996) *Oncogene 12*, 125−133.
16. Darnell, J. E. (1997) *Science 277*, 1630−1635.
17. Li, X., Leung, S., Quereshi, S., Darnell, J. E., and Stark, G. R. (1996) *J. Biol. Chem. 271*, 5790−5794.
18. Farrar, J. D., Smith, J. D., Murphy, T. L., and Murphy, K. M. (2000) *J. Biol. Chem. 275*, 2693−2697.
19. Shuai, K., Horvath, C. M., Huang, L. H. T., Qureshi, S. A., Cowburn, D., and Darnell, J. E. (1994) *Cell 76*, 821−828.
20. Nadeau, O. W., Domanski, P., Usacheva, A., Uddin, S., Platanias, L. C., Pitha, P., Raz, R., Levy, D., Majchrzak, B., Fish, E., and Colamonici, O. R. (1999) *J. Biol. Chem. 274*, 4045−4052.
21. Li, X., Leung, S., Kerr, I. M., and Stark, G. R. (1997) *Mol. Cell. Biol. 17*, 2048−2056.
22. Nguyen, V.-P., Saleh, A. Z. M., Arch, A. E., Yan, H., Piazza, F., Kim, J., and Krolewski, J. J. (2002) *J. Biol. Chem. 277*, 9713−9721.
23. Colamonici, O. R., Yan, H., Domanski, P., Handa, R., Smalley, D., Mullersman, J., Witte, M., Krishnan, K., and Krolewski, J. J. (1994) *Mol. Cell. Biol. 14*, 8133−8142.
24. Vinkemeier, U., Cohen, S. L., Moarefi, I., Chait, B. T., Kuriyan, J., and Darnell, J. E. (1996) *EMBO J. 15*, 5616−5626.
25. Chen, X., Vinkemeier, U., Zhao, Y., Jeruzalmi, D., Darnell, J. E., and Kuriyan, J. (1998) *Cell 93*, 827−839.
26. Krishnan, K., Singh, B., and Krolewski, J. J. (1998) *J. Biol. Chem. 273*, 19495−19501.
27. McTigue, M. A., Williams, D. R., and Tainer, J. A. (1995) *J. Mol. Biol.* 21−27.
28. Becker, S., Corthals, G. L., Aebersold, R., Groner, B., and Müller, C. W. (1998) *FEBS Lett. 441*, 141−147.
29. Johnsson, B., Lofas, S., and Lindquist, G. (1991) *Anal. Biochem. 198*, 268−277.
30. Schuck, P. (1997) *Annu. Rev. Biophys. Biomol. Struct. 26*, 541−566.
31. Roden, L. D., and Myszka, D. G. (1996) *Biochem. Biophys. Res. Commun. 225*, 1073−1077.
32. Panayotou, G., Gish, G., End, P., Truong, O., Gout, I., Dhand, R., Fry, M. J., Hiles, I., Pawson, T., and Waterfield, M. D. (1993) *Mol. Cell. Biol. 13*, 3567−3576.
33. Ladbury, J. E., Lemmon, M. A., Zhou, M., Green, J., Botfield, M. C., and Schlessinger, J. (1995) *Proc. Natl. Acad. Sci. U.S.A. 92*, 3199−3203.
34. Greenlund, A. C., Morales, M. O., Viviano, B. L., Yan, H., Krolewski, J., and Schreiber, R. D. (1995) *Immunity 2*, 677−687.

BI025913F